THE JOURNAL OF BIOLOGICAL CHEMISTRY VOL. 282, NO. 35, pp. 25464–25474, August 31, 2007

siRNA Screening of the Kinome Identifies ULK1 as a Multidomain Modulator of Autophagy*[S]

Received for publication, May 3, 2007, and in revised form, June 25, 2007 Published, JBC Papers in Press, June 26, 2007, DOI 10.1074/jbc.M703663200

Edmond Y. W. Chan, Serkan Kir, and Sharon A. Tooze[1]

From the Secretory Pathways Laboratory, Cancer Research UK London Research Institute, London WC2A 3PX, United Kingdom

Autophagy is a vital response to nutrient starvation. Here, we screened a kinase-specific siRNA library using an autophagy assay in human embryonic kidney 293 cells that measures lipidation of the marker protein GFP-LC3 following amino acid starvation. This screen identified *ULK1* in addition to other novel candidates that could be confirmed with multiple siRNAs. Knockdown of *ULK1*, but not the related kinase *ULK2*, inhibited the autophagic response. Also, *ULK1* knockdown inhibited rapamycin-induced autophagy consistent with a role downstream of mTOR. Overexpression of ULK1 inhibited autophagy and this inhibition was independent of its kinase activity. Deletion of the PDZ domain-binding Val-Tyr-Ala motif at the ULK1 C terminus generated a more potent dominant-negative protein. Further deletions revealed that the minimal ULK1 dominant-negative region could be mapped to residues 1–351. Full-length ULK1 localized to cytoplasmic structures, some of which were GFP-LC3-positive, and this localization required the conserved C-terminal domain. In contrast, ULK1-(1–351) was diffuse in the cytoplasm. These experiments reveal at least two domains in ULK1 which likely function via unique sets of effectors to regulate autophagy.

During macroautophagy, a membrane cisterna wraps around cytoplasmic material to form a nascent autophagosome, which subsequently fuses with degradative endosomes. The targets of autophagy can include long-lived proteins, damaged organelles, ubiquitinated cellular substrates, and aberrant protein aggregates (1–4). Macroautophagy, which we refer to here as autophagy, is rapidly induced in response to amino acid deprivation and acts to recycle free molecular building blocks to the starving cell. Reflecting this cellular metabolic role, autophagy also appears to be critical in the maintenance of proper nutritional balance in the context of neonatal mice, developing *Dictyostelium*, and *Caenorhabditis elegans* undergoing development arrest (1, 5–7). Autophagy is also a major component of type-II non-apoptotic programmed cell death, and this may form part of the response to certain types of cell stress (8–12). The recent implication of autophagy in medical contexts such as cancer, neurodegeneration and immunity have increased interest in elucidating the basic molecular mechanisms of the process (4, 13–16).

Two yeast screens pioneered the identification of molecular components required for autophagy and a unified nomenclature has been devised for these genes (17–19). Although the function for many of these genes is unknown, a large proportion can be grouped into distinct biochemical pathways. Studies in yeast and mammalian cells have established the stepwise progression of these pathways, which appear to be essential at an early stage of autophagy (20, 21). For example, the gene products of *Atg3*, *Atg4*, *Atg5*, *Atg7*, *Atg8*, *Atg10*, *Atg12*, and *Atg16* function coordinately in two interrelated ubiquitin-like conjugation systems (22–24). Importantly, yeast Atg8p and its mammalian homologs become covalently linked to a phospholipid upon the induction of autophagy. This conversion of Atg8 proteins from their unlipidated species (also known as form-I) to the lipidated species (form-II) helps direct autophagosome formation by a poorly understood mechanism that appears to involve translocation of Atg8-II onto pre-autophagosomal membranes (24, 25). We and others have shown that the green fluorescent protein (GFP)[2]-tagged mammalian Atg8 homolog microtubule-associated protein light chain 3 (LC3), when stably expressed, is an effective marker protein for monitoring the lipidation reaction and membrane translocation (25–28).

Another complex essential for autophagy in yeast involves the protein kinase Atg1p and its interacting protein Atg13p, which have been shown to function downstream of target of rapamycin (TOR) and the Ras/PKA pathway (29, 30). Studies performed using *Dictyostelium*, *Drosophila*, and *C. elegans* have confirmed a role for their *Atg1* homologs in autophagy (6, 7, 31, 32). In mammals, two *Atg1* homologs have been identified, uncoordinated 51-like kinase 1 (*ULK1*) and *ULK2* (33, 34), and we recently demonstrated an involvement of ULK1 in the subcellular re-distribution of mammalian Atg9 that takes place following nutrient starvation (35). Evidence from *Drosophila* and mammalian cells also indicate that Atg1 proteins have the ability to signal "upstream" to TOR via a feedback loop (32, 36). Additionally, it was recently shown that ULK1 can be ubiquitinated and enter into a complex containing the polyubiquitin-binding protein p62 and TrkA NGF receptor, although the

* The costs of publication of this article were defrayed in part by the payment of page charges. This article must therefore be hereby marked "*advertisement*" in accordance with 18 U.S.C. Section 1734 solely to indicate this fact.
[S] The on-line version of this article (available at http://www.jbc.org) contains supplemental Tables S1 and S2 and Figs. S1–S6.
[1] To whom correspondence should be addressed: Secretory Pathways Laboratory, Cancer Research UK London Research Institute, 44 Lincoln's Inn Field, London WC2A 3PX, UK. Tel.: 44-0-207-269-3045; E-mail: Sharon.Tooze@cancer.org.uk.

[2] The abbreviations used are: GFP, green fluorescent protein; DMEM, Dulbecco's modified Eagle's medium; FBS, fetal bovine serum; TOR, target of rapamycin; LC3, light chain 3; ULK, uncoordinated 51-like kinase.

function of this pathway in autophagy is currently unknown (37).

Here, we searched for autophagy regulators by performing siRNA-based functional genomics in a human cell line model for autophagy. To screen for signal transduction pathways, we used a 753-member "kinome" library designed to target all known and predicted human kinases and some associated subunits. Our screen utilized a biochemical immunoblotting assay for GFP-LC3 conversion and candidates were confirmed using multiple assays for autophagy. In addition to novel candidates, the screen also identified ULK1, but not ULK2, as an autophagy regulator. We used overexpression studies to define regions in ULK1 regulating autophagy and regions controlling the localization of ULK1 to autophagic structures. The analysis of these non-overlapping but complementary domains in ULK1 provide evidence for multiple functional modules in ULK1.

EXPERIMENTAL PROCEDURES

Cell Culture—293A cells stably expressing EGFP-rat LC3 have been described before (27). HeLa cells were provided by E. L. Eskelinen (University of Helsinki, Finland). Both cell types were maintained in DMEM/10% FBS, and this also served as full nutrient medium in the analytical experiments.

siRNA Transfections—The siRNA library contained SMART pools (Dharmacon) of 4 siRNA duplexes per gene targeting 753 protein kinases, lipid kinases, and regulatory subunits (see supplemental Table S2). SMART pool siRNA was also obtained for the human homologs of *Atg5* (NM_004849), *Atg7* (NM_006395), *Atg12* (NM_004707), and *ULK2* (NM_014683). Negative control siRNA was either the siControl non-targeting pool (that contains 4 duplexes) (Dharmacon), or (in the case of the library screen) a pool of 2 scrambled duplexes that have been routinely used in the laboratory (corresponding to sequences 5′-U ACC UUU AGC AUG AUG UGU-3′ and 5′-A UAA UGU GAC GAA UGA UCC). Sequences of the individual duplexes for chosen candidates are presented in supplemental Fig. S5. For the screen, 293/GFP-LC3 cells were seeded in 96-well dishes and transfected with 50 nM final siRNA using Oligofectamine reagent (Invitrogen Life Sci) according to the manufacturer's protocols. Forty-eight hours after siRNA treatment, full nutrient medium was replenished. Then, following an additional 24 h, autophagy was initiated by incubating cells for 2 h in Earle's balanced saline solution (EBSS) (containing 0.5 mM leupeptin where indicated). Cell extracts were prepared in lysis buffer (150 mM NaCl, 20 mM Tris pH 7.5, 5 mM EDTA, 0.3% v/v Triton X-100 containing the Complete EDTA-free protease inhibitor mixture (Roche Applied Science)), mixed with SDS-sample buffer and analyzed using 10% SDS-PAGE. For control experiments (analyzing knockdown of Atg genes), and all other experimental tests, the format was scaled into 12- or 24-well dishes to minimize cell loss and reduce sample variability.

Immunoblotting—To detect GFP-LC3, proteins were transferred to polyvinylidene difluoride membranes and probed with a mixture of anti-GFP rabbit polyclonal antibody SG5 (from Dr. T. Hunt, Cancer Research UK, London) and anti-actin mouse monoclonal AC40 antibody (Sigma). Signals were quantified using secondary antibodies coupled to infrared chromophores and a 2-channel scanning method (Licor). Additionally, polyclonal antibody for phospho-S6 protein was obtained from Cell Signaling Technologies. Anti-β COP polyclonal and anti-MYC monoclonal 9E10 antibodies were obtained from Cancer Research UK.

Confirmation of Knockdown by RT-PCR—Cell samples following 48 h of knockdown were lysed in TRIzol reagent (Invitrogen) for isolation of total RNA. First strand cDNA was synthesized using oligo dT primer and Superscript II enzyme (Invitrogen). PCR primers for each candidate gene or actin were designed off 3′-regions of the cDNA sequences (spanning multiple exons), and these primers were used in real time PCR reactions performed with SYBR green chemistry (Applied Biosystems). Fold decreases in mRNA levels were determined after calibration of the assay using standard curve methods.

Overexpression of ULK1—Expression plasmids for wild-type and kinase-dead (K46R) murine ULK1 have been described (38). Constructs used here containing an N-terminal Myc epitope tag, and various deletions were derived from these. For biochemical analysis by GFP-LC3 conversion or protein degradation, cells were transfected with high efficiency and high expression levels using Lipofectamine 2000 (Invitrogen) according to the manufacturer's protocols. For analysis of protein localization on glass coverslips, lower expression levels were achieved using FuGENE 6 (Roche Applied Sciences) transfection reagent. In all cases, 24 h after transfection, cells were starved for 2 h and then lysed or fixed for analysis.

Microscopic Analysis of GFP-LC3 Translocation—293/GFP-LC3 cells were seeded onto glass coverslips and 24 h later transfected with 25 nM final siRNA. Forty-eight hours after siRNA treatment, full nutrient medium was replenished, and then, after an additional 24 h, autophagy was induced by starvation in EBSS/0.5 mM leupeptin. After 120 min of induction, cells were fixed with paraformaldehyde, briefly stained with 4′,6-diamidino-2-phenylindole (DAPI), and then mounted onto glass slides. Cells were visualized using a 20×-0.75 N.A. air objective and a Hamamatsu 12-bit camera mounted on a Discovery-1 automated microscope (Molecular Devices). Multiple fields at random positions were collected for each condition. Automated quantification of GFP-LC3-labeled structures in the images was performed using the Granularity algorithm of the Metamorph 6.2 software package (Molecular Devices) using equivalent settings between the various conditions.

Protein Degradation—293/GFP-LC3 or HeLa cells were seeded in 6-well dishes and transfected with siRNA or expression plasmid as described above. Forty-eight hours after siRNA treatment, or 8 h after plasmid transfection, cells were exchanged into labeling medium (DMEM/10% dialyzed FBS containing [^{14}C]valine (0.2 μCi/ml) in 65 μM unlabeled valine) and incubated overnight. The following day, cells were exchanged into chase medium (DMEM/10% FBS/2 mM unlabeled valine) and further incubated for 4 h to remove the contribution of short-lived proteins. After the chase period, cells were exchanged into EBSS/2 mM valine to initiate autophagy, and following 2 h of induction, the media were collected, and the trichloroacetic acid-soluble fraction was analyzed by scintillation counting. The cells were lysed in ice-cold phosphate-buffered saline containing 1% Triton X-100 and the trichloro-

acetic acid-insoluble fraction of this was isolated, resolublized in 9 M urea, and then counted to obtain a measurement of total cellular labeling. Autophagy was quantified as percentage of protein degradation, which was calculated using ((medium trichloroacetic acid-soluble counts)/(medium trichloroacetic acid-soluble counts) + (cellular trichloroacetic acid-insoluble cellular counts)). We typically observed ~4% degradation (over 2 h) in control starved cells, which is in agreement with previous studies (27, 39–41) and experimental data were normalized to their corresponding control value to allow comparison across independent experiments.

Statistical Analysis—In the screen raw data, there is variability in the GFP-LC3 ratio (calculated as GFP-LC3-II/(GFP-LC3-I + GFP-LC3-II)) that can be attributed most likely to the immunoblotting technique. To compare library data from multiple blots, we used a normalization process whereby the GFP-LC3 ratios of each blot were adjusted by a constant value until the median GFP-LC3 ratios from each blot were equivalent. This process is described in greater detail in supplemental Fig. S2. To calculate *p* values for the adjusted pooled GFP-LC3 ratio data, we used an empirical Bayes *t* test, which compensates for the small replicate numbers by moving an individual gene variance toward a consensus (across all genes) variance (42). For other analyses, we calculated *p* values between groups using the Student's *t* test for data sets with two-tailed distributions and equal variance.

RESULTS

Screen of Human Kinome for Autophagy Modulators—To identify novel regulators of autophagy, we screened a siRNA library which targets 753 human kinases and regulatory subunits. As our model system, we used HEK 293 cells stably expressing the GFP-LC3 marker protein (293/GFP-LC3), which have previously been shown to rapidly respond to starvation induced autophagy by morphological and biochemical assays (27). We used 293 cells as they are targeted very efficiently by siRNAs. Even with siRNA concentrations as low as 5 nM in the final transfection mixture, total protein levels can be reduced as much as 90% (27) and >90% of cells are targeted (data not shown).

Autophagy is induced through amino acid starvation of cells by incubation in Earle's buffered saline solution (EBSS) for 2 h, which therefore also results in serum starvation. We observed in 293 cells that the presence or absence of serum does not affect the activation of autophagy, at least as detected using GFP-LC3 (data not shown). For all GFP-LC3 conversion experiments, the lysosomal protease inhibitor leupeptin was also included in the starvation medium to decrease autophagosomal degradation and enhance the accumulation of the lipidated GFP-LC3-II. To validate our model system, we analyzed siRNAs for various human Atg genes and we observed in 293/GFP-LC3 cells that knockdown of *Atg5*, *Atg7*, and *Atg12* had the strongest inhibitory effects on GFP-LC3 conversion (Fig. 1*A*). Atg7 is the ubiquitination E1-like enzyme that catalyzes LC3 conversion. Atg7 also catalyzes the Atg5–Atg12 conjugation event that is prerequisite for LC3 conversion (21).

Each gene in our library was targeted by a pool of 4 different siRNA duplexes and for the screen, each gene was analyzed in

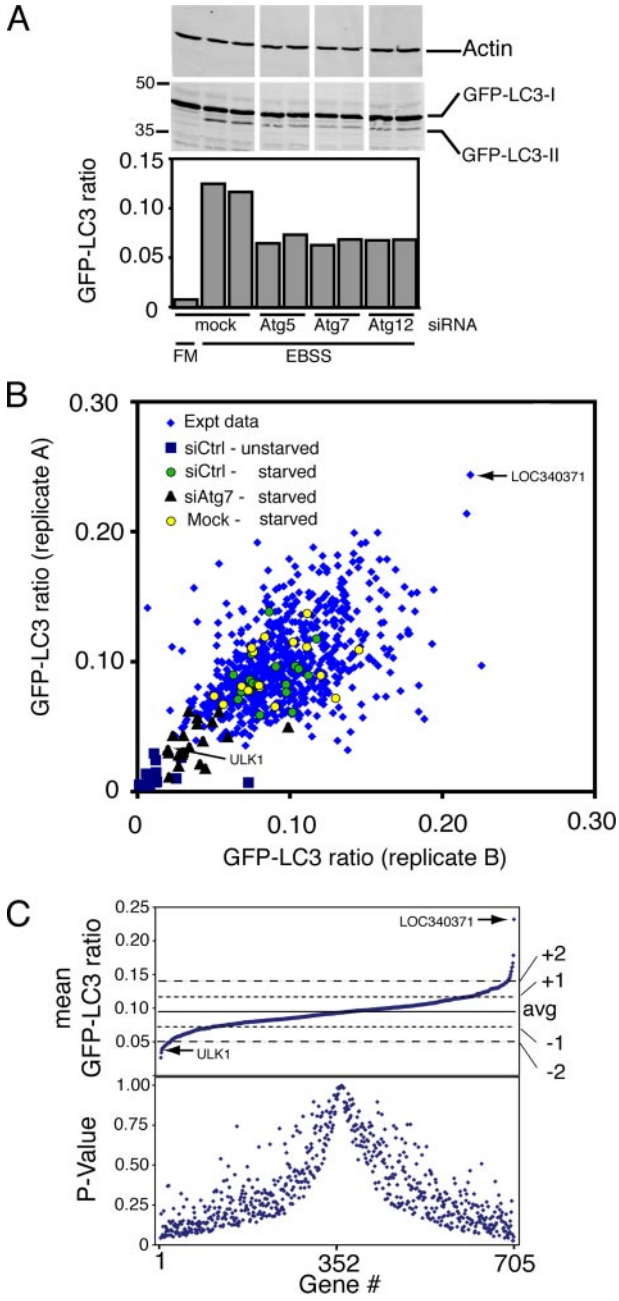

FIGURE 1. **Screen of the human kinome for modulators of autophagy in 293A cells stably expressing GFP-LC3.** *A*, inhibition of GFP-LC3 conversion by siRNAs targeting known *Atg* genes. 293/GFP-LC3 cells were transfected with siRNA pools (50 nM final) designed to target the human homologs of *Atg5*, *Atg7*, and *Atg12* using duplicate cell samples. 72 h after transfection, cells were incubated in EBSS containing leupeptin (EBSS) for 2 h, and then harvested. *Top panels*, cell lysates resolved by SDS-PAGE were immunoblotted with anti-actin and anti-GFP antibodies and then quantitatively analyzed. *Bottom*, quantification of the GFP-LC3 conversion ratio (GFP-LC3-II/(GFP-LC3-I + GFP-LC3-II)). The first lane is the control unstarved cell sample that was maintained in full nutrient medium (*FM*). *B*, the siRNA kinome library targeting 705 genes was analyzed in duplicate using the SDS-PAGE assay for GFP-LC3 conversion. Each gene of the library is represented by one experimental data point with the X and Y coordinates corresponding to the GFP-LC3 conversion ratios in the replicate experiments. The mock-transfected, *Atg7* siRNA and non-targeting siRNA internal controls from each immunoblot are also shown. See supplemental Fig. S1 for an example of raw immunoblot data from the screen. *C*, distribution of all adjusted (see "Experimental Procedures" and supplemental Fig. S2 for details of adjustment method) GFP-LC3 scores. *Top*, 705 genes studied in the library were sorted based on their mean adjusted GFP-LC3 ratio scores. The positions of the average score ± 1 or 2 S.D. are shown on the *right*. *Bottom*, for every gene, its corresponding *p* value is plotted (at the same position on the X-axis). In *B* and *C*, the positions of the screen candidates *ULK1* and *LOC340371* are indicated.

duplicate to obtain quantitative scores for GFP-LC3 conversion. This duplicate analysis was contained within 40 separate immunoblotted SDS-PAGE gels and each gel included non-targeting and *Atg7* siRNA internal controls. An example of primary data is presented in supplemental Fig. S1. Fig. 1*B* shows the general range and correlation between the replicate experimental data sets and their relation to the internal controls. Of the 753 genes initially included in the screen, 48 (6%) were lost during culturing or could not be analyzed in one of the replicates. To accurately compare the remaining 705 genes across the multiple immunoblots, GFP-LC3 conversion ratios were corrected so that the median value on each blot was equal among all blots (see supplemental Fig. S2). The average GFP-LC3 conversion ratios for each gene were ranked, and 96% of the scores fell within 2 standard deviations from the mean value over the entire library (Fig. 1*C*). Taking into account the duplicate data sets, p values were derived for each gene. As expected, the p values decreased for genes showing the greatest effects on GFP-LC3 conversion. For further confirmatory experiments, we focused on 12 representative candidates with $p < 0.06$, which also showed the most dramatic fold changes (supplemental Table S1). Other than *ULK1*, no other candidate had a described link with autophagy. A total list of genes included the library is provided in supplemental Table S2.

Several genes were absent from our initial list of screen candidates including PI 3-kinases and components of the mTOR-p70S6 kinase signaling pathway that have been implicated in autophagy regulation (29, 43, 44). In follow-up experiments, we observed that knockdown of the *hVps34* class III PI 3-kinase did not strongly inhibit GFP-LC3 conversion in our cell model, despite the clear sensitivity of GFP-LC3 conversion to the PI3 kinase inhibitor wortmannin (supplemental Fig. S3). Additionally, we re-confirmed our screen results that knockdown of *mTOR* or any single *p70S6 kinase* gene did not increase levels of GFP-LC3 conversion following starvation (or under full nutrient conditions) (supplemental Fig. S4) despite the sensitivity of the assay to rapamycin (see Fig. 4*E*). However, knockdown of both *p70S6 kinase* genes together decreased starvation-dependent GFP-LC3 conversion.

Confirmation of Candidate Individual siRNAs—Because siRNA screens in mammalian cells can potentially be influenced by interfering off-target effects (45), we re-confirmed the top candidates by studying the 4 individual duplexes of the SMART pools. Our criteria for specificity were that: 1) at least 2 of the individual siRNAs should confirm the modulatory effect on GFP-LC3 conversion as observed using siRNA pools, and 2) knockdown of the transcript by the individual siRNAs can be confirmed. 7 of 12 candidates re-screened fit these criteria (Fig. 2). All 4 duplex sequences for the candidate *LOC340371* gave similar stimulatory effects on GFP-LC3 conversion; 3 duplexes were identified for *MAP2K6* that produced inhibitory effects; and 2 duplexes were identified for the candidates *ULK1*, *HUNK*, *ROCK1*, *CDK8*, and *SGK1* which produced internally consistent modulatory effects. Sequences corresponding to the siRNA duplexes that were confirmed are listed in supplemental Fig. S5.

Modulation of Autophagic Protein Degradation—To characterize the candidates using an autophagy assay independent of

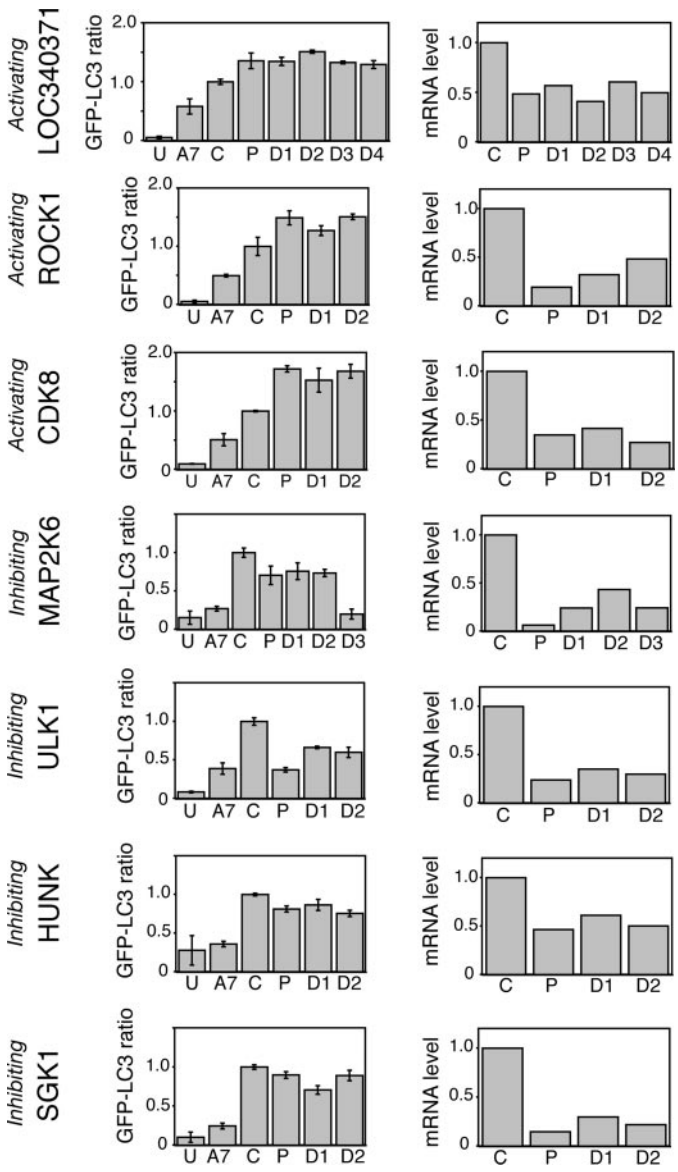

FIGURE 2. **Confirmation of individual siRNA duplexes for candidate genes that modulate autophagy.** 293/GFP-LC3 cells were transfected with: a siRNA pool toward *Atg7* (*A7*); control non-targeting siRNA (*C*); a pool of 4 individual siRNA duplexes targeting the candidate gene (*P*); or each siRNA duplex individually (*D1–D4*). Shown are the data for genes that have 2 or more individual duplexes that confirm the primary screening data. Candidates are grouped as either having activating or inhibiting effects on GFP-LC3 conversion. *A7*, negative-control (*C*) and pooled (*P*) siRNAs were used at 50 nM final concentration, while D1–D4 duplexes were used at 12.5 nM. *Left panels*, 72 h after transfection, cells were starved in EBSS/leupeptin and analyzed for GFP-LC3 conversion as in Fig. 1*A*. Each column represents three replicates ± S.D. GFP-LC3 ratios have been normalized to the starved-control siRNA-treated cells (*C*). *U*, control unstarved cells. *Right panels*, cell samples knocked down in parallel were analyzed by quantitative realtime RT-PCR. Data are expressed as relative amount of mRNA for the target gene normalized to actin mRNA levels.

GFP-LC3, we measured rates of starvation-induced long-lived protein degradation in [^{14}C]valine-labeled cells (40, 46). Autophagic protein degradation could be inhibited to uninduced levels by the addition of either wortmannin or leupeptin to the EBSS starvation medium, while, in contrast, the proteasomal inhibitor lactacystin did not show any inhibition (data not shown). *ULK1* knockdown inhibited protein degradation, both in the basal state and more obviously, following amino acid

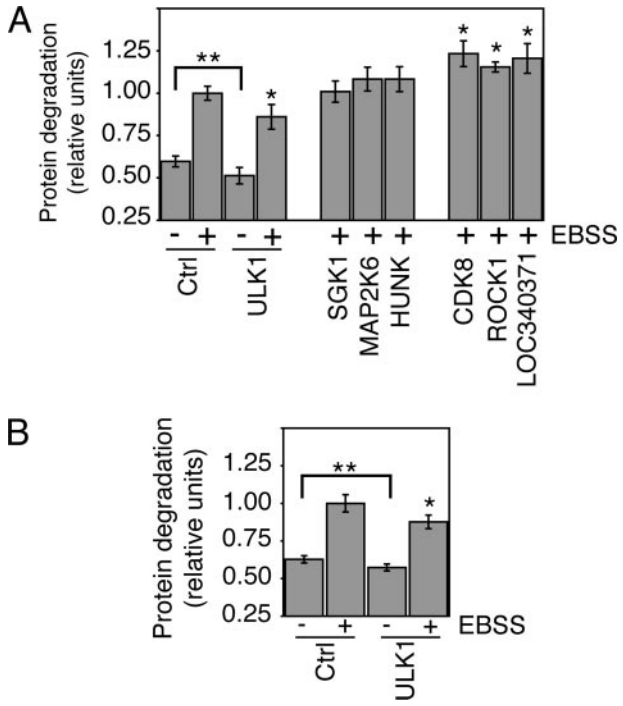

FIGURE 3. **Modulation of starvation-induced long-lived protein degradation by siRNAs for candidate genes.** *A*, 293/GFP-LC3 cells were transfected with negative-control siRNA (*Ctrl*) or siRNA pools (50 nM) as indicated. After 48 h of knockdown, cells were labeled with [^{14}C]valine overnight. The following day, autophagy was induced by starvation in EBSS (without leupeptin) as indicated, and protein degradation was measured as described under "Experimental Procedures." *B*, HeLa cells were transfected with siRNAs and assayed for autophagic protein degradation as described in *A*. Values are expressed as relative units after normalization to the control knockdown starved sample. Each column reports the average of six measurements (±S.D.) derived from two independent experiments. *, $p < 0.002$ as compared with starved siCtrl sample. **, $p < 0.003$ as compared with unstarved-siCtrl sample.

starvation (Fig. 3*A*). This requirement of *ULK1* for efficient protein degradation was also observed following knockdown in HeLa cells (Fig. 3*B*). For the other candidates, we could confirm that knockdown of *CDK8*, *ROCK1*, or *LOC340371* significantly increased levels of starvation-induced protein degradation. However, knockdown of *CDK8*, *ROCK1*, or *LOC340371* did not significantly increase basal autophagy in the unstarved state as determined by GFP-LC3 conversion and knockdown of these genes did not inhibit the ability of nutrients to promote phosphorylation of p70 S6 kinase and ribosomal S6 protein (data not shown). Knockdown of *SGK1*, *MAP2K6*, or *HUNK* did not reduce levels of protein degradation, as would have been predicted based on the inhibition of GFP-LC3-II. Further experiments are needed to explore *CDK8*, *ROCK1*, *LOC340371* and remaining candidates. Another candidate, *PRKAR1A*, which was initially not chosen for further studies because its *p* value just failed to meet the cut-off, was recently corroborated by the finding that autophagosome formation was reduced in *PRKAR1A*$^{-/-}$ MEFs (47).

Regulation of Autophagy by ULK1—Both ULK1 and ULK2 share homology to yeast Atg1p and both were assayed in the initial kinome screen. However, only ULK1 was recovered as a candidate. We reconfirmed that knockdown of *ULK2* did not modulate starvation-induced GFP-LC3 conversion, despite properly targeting the mRNA (Fig. 4, *A–C*). Together, these data suggest that ULK1 is the functional homologue of Atg1p, at least in our cell model, and is the primary autophagy regulator in mammalian cells.

In yeast, Atg1p has been shown to play a critical role in autophagy downstream of TOR, and this function requires a differential binding to Atg13p in a rapamycin-regulated manner (29). Because it was unclear how much of the yeast mechanism is conserved in mammals, we investigated the relationship of ULK1 and mTOR in 293 cells. As expected, starvation of 293/GFP-LC3 cells in EBSS/leupeptin caused an inhibition of mTOR-p70S6 kinase signaling (as detected by ribosomal protein S6 phosphorylation) and stimulated the conversion of GFP-LC3 (Fig. 4*D*). In cells following knockdown of *Atg7* or *ULK1*, starvation caused a similar depression in mTOR-p70S6 kinase signaling, although now, GFP-LC3 conversion was largely inhibited. Knockdown of *ULK1* similarly inhibited GFP-LC3 conversion following incubation of cells with rapamycin in full nutrient medium, although rapamycin still clearly inhibited mTOR (Fig. 4*E*). Thus, in 293 cells, ULK1 also appears to function at a step downstream of mTOR in regulating autophagy.

In 293/GFP-LC3 cells, autophagy can also be monitored by the formation of cytoplasmic autophagosomes decorated by GFP-LC3 following amino acid starvation (27) or rapamycin treatment. Transfection with negative control siRNA did not inhibit the formation of GFP-LC3-positive structures following 2 h of starvation in EBSS/leupeptin (Fig. 4*F*). Knockdown of *ULK1* inhibited the formation of autophagosomes labeled with GFP-LC3 to similar levels as knockdown of *Atg7* (Fig. 4*G*). *ULK1* knockdown similarly inhibited the formation of rapamycin induced GFP-LC3-positive autophagosomes (data not shown). These results demonstrate that ULK1 is the functionally equivalent mammalian homologue of the yeast Atg1p.

Inhibition of Autophagy by Overexpressed ULK1—ULK1 contains an N-terminal kinase domain, an internal region rich in Ser and Pro residues, and a C-terminal region that is relatively more conserved (33, 38) (Fig. 5*A*). Overexpression of DmAtg1 in cells of the *Drosophila* fat body and imaginal discs was recently shown to activate autophagy, even under full nutrient conditions (32). Therefore, to begin to investigate the role of ULK1 in mammalian cell autophagy, we used a similar approach. In contrast to the results in *Drosophila*, we found that overexpression of Myc-tagged wild-type ULK1 in normally fed 293/GFP-LC3 cells did not stimulate GFP-LC3 conversion (data not shown) or autophagic protein degradation (Fig. 5*B*). In fact, we observed that ULK1 overexpression mildly inhibited starvation-induced GFP-LC3 conversion and protein degradation. To investigate this effect further, we transfected varying amounts of ULK1 and observed that the severity of inhibition on GFP-LC3 conversion correlated with levels of overexpression (Fig. 5*C*). ULK1 containing a Lys to Arg mutation at position 46 (K46R) has been shown to lack kinase activity (38). Overexpression of K46R ULK1 produced a dosage-dependent inhibition of GFP-LC3 conversion similar to wild-type ULK1, suggesting that the inhibitory mechanism for full-length ULK1 may be kinase-independent.

Domain Mapping Reveals a Bipartite Signal in ULK1—To determine which domain of ULK1 when overexpressed inhibits autophagy, we expressed truncations of ULK1 in 293

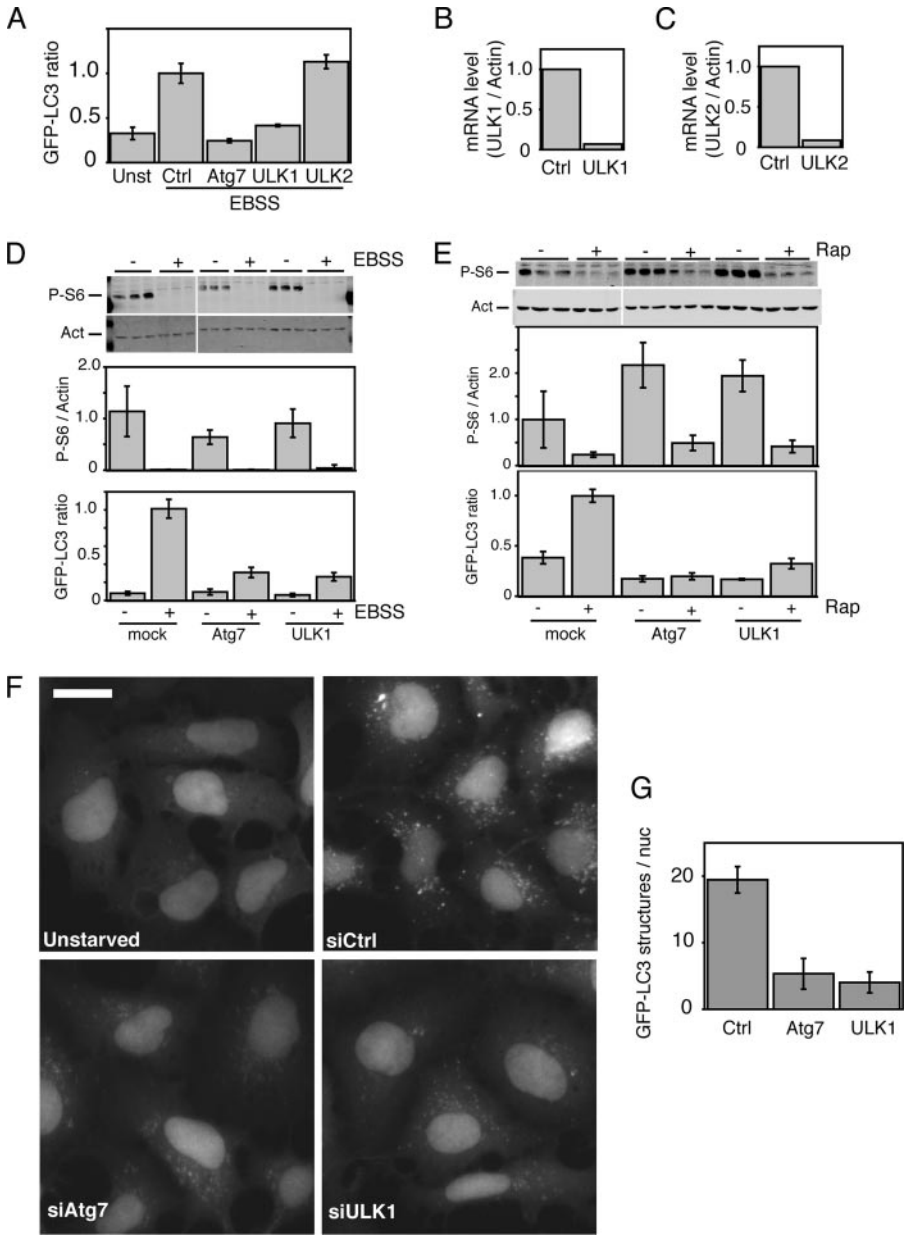

FIGURE 4. **ULK1 is required for autophagy.** 293/GFP-LC3 cells were transfected with siRNA pools as indicated for 72 h. *A*, cells were then left unstarved (*Unst*) or starved in EBSS/leupeptin (*EBSS*) for 2 h and analyzed for GFP-LC3 conversion. *B* and *C*, parallel samples were analyzed by quantitative RT-PCR. Data are normalized to actin mRNA levels. *D* and *E*, 293/GFP-LC3 cells were transfected with siRNA pools targeting *Atg7* or *ULK1* for 72 h. Cells were then either: *D*, starved for 2 h or *E*, treated with rapamycin (*Rap*) (50 μg/ml) for 30 min as indicated and then lysed for analysis by SDS-PAGE. In addition to assessing GFP-LC3 conversion, phosphorylation levels on ribosomal protein S6 (*P-S6*) were quantified and normalized to actin levels. *F*, 293/GFP-LC3 cells were transfected with negative control siRNA (*siCtrl*) or siRNA pools toward *Atg7* or *ULK1* and, 72 h later, starved in EBSS/leupeptin for 2 h. Cells were then visualized using wide-field epifluorescent microscopy. Unstarved cells show low numbers of GFP-LC3 puncta as compared with control-siRNA-transfected cells that have been starved (*siCtrl*). Knockdown of *Atg7* or *ULK1* reduces the number of GFP-LC3-positive structures. *Scale bar*, 20 μm. *G*, GFP-LC3-positive structures were quantitated using image analysis software. Values are represented as number of puncta (with GFP signal greater than a fixed threshold intensity)/cell. Each column reports 6–8 fields ± S.D. Between 600–1000 cells were quantitated per column. Images shown in *F* comprised ~10% of a whole microscopy field.

cells and assayed for GFP-LC3 conversion. The highly conserved 222-residue C-terminal domain (CTD) of mammalian ULK1 is known to bind SynGAP, which regulates the GTPases Ras and Rab5, and this binding is disrupted upon deletion of the ULK1 C-terminal 50 residues (48). The CTD was also shown to bind the PDZ domain containing protein Syntenin1, another potential Rab5 regulator, and this interaction is entirely dependent upon the Val-Tyr-Ala (VYA) PDZ-binding motif at the ULK1 C terminus (48).

Expression of ULK1 lacking its CTD (ΔCTD) resulted in a greater inhibition of GFP-LC3 conversion than expression of comparable amounts of the wild-type protein (Fig. 5, *C* and *E*). In addition, overexpression of ULK1ΔCTD inhibited autophagic protein degradation to levels observed in unstarved cells (Fig. 5*D*). Surprisingly, ULK1 with shorter deletions of the CTD (ULK1Δ50) or deletion of the C-terminal PDZ-domain-binding motif (ULK1ΔVYA) inhibited starvation-induced GFP-LC3 conversion as robustly as the ULK1ΔCTD mutant (Fig. 5*E*). Thus, deletion of the C-terminal 3 amino acids is sufficient to markedly alter the autophagy regulatory functions of ULK1.

To identify a minimal dominant inhibitory region, we made additional ULK1 deletion constructs. Previously, it was shown using pull-down and yeast two-hybrid systems that a region of ULK1 roughly encompassing residues 279–427 can bind GATE-16 and GABARAP, two other homologs of yeast Atg8 (49). However, additional deletion analysis demonstrated that ULK1 residues 352–427 was critically required for binding to GATE-16 and GABARAP. Here, we found that both 1–427 or 1–351 ULK1 deletion mutants retained ability to robustly inhibit starvation-dependent GFP-LC3 conversion (Fig. 5*G*). In contrast, the 1–278 truncation mutant, which only contains the ULK1 kinase domain, did not display dominant-negative effects (Fig. 5*F*).

Localization of ULK1 to GFP-LC3-positive Structures—In yeast, Atg1p clearly localizes to the pre-autophagosome structure (PAS), a unique site where multiple Atg proteins organize to synthesize nascent autophagosomes (20, 30, 50). The originating membrane source of mammalian autophagosomes is thought to reside in multiple structures that have transient associations with Atg5, and more a stable association with Atg8 homologs such as LC3 and mammalian Atg9 (21, 35). To characterize the

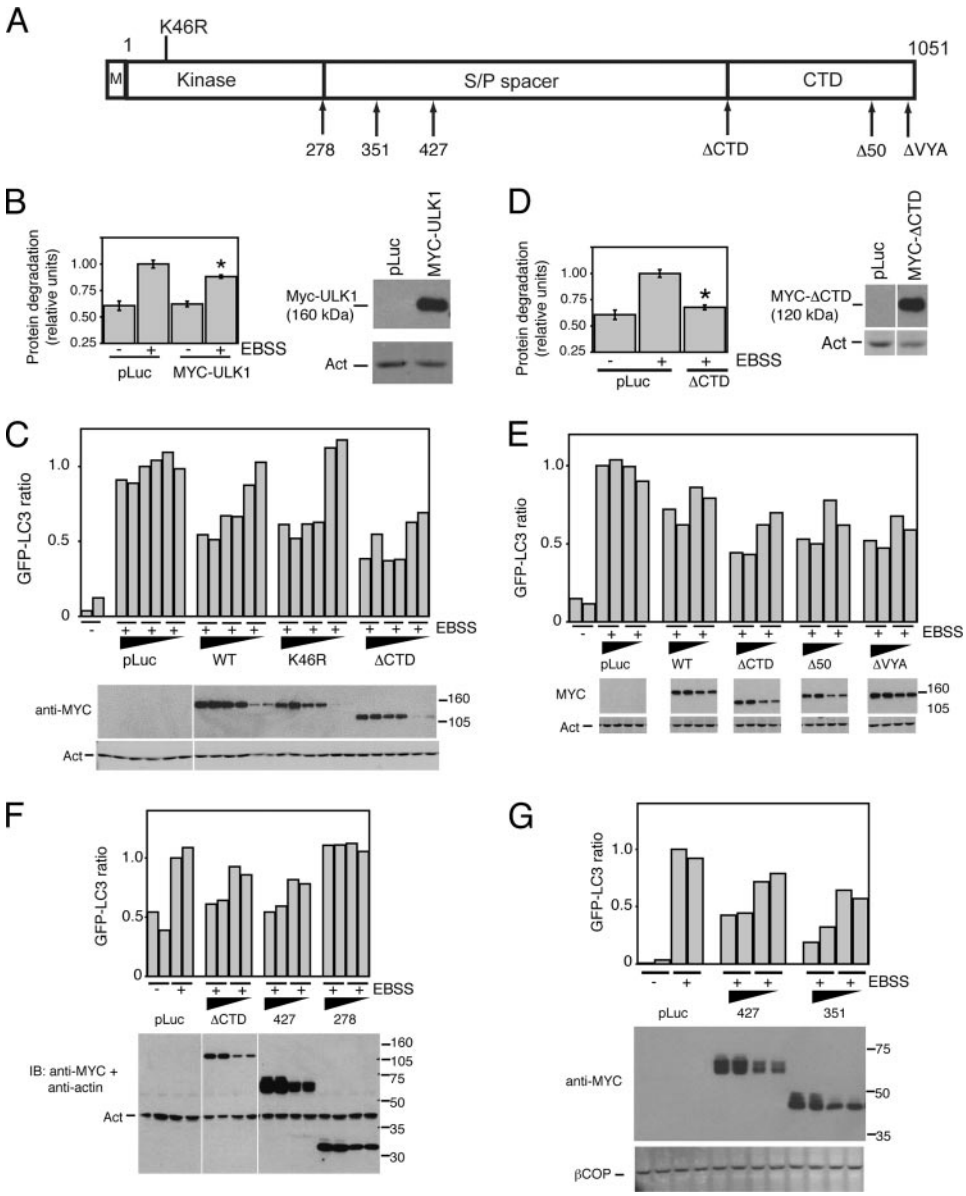

FIGURE 5. **Residues 1–351 of ULK1 contain potent inhibitory function.** *A*, domain map of murine ULK1 showing positions of the Myc tag (*M*), kinase domain, Ser/Pro-rich spacer domain, and conserved C-terminal domain (*CTD*). Below the diagram are positions of stop codons inserted to generate the various deletion constructs. *B*, *left*, 293/GFP-LC3 cells were transfected with either negative control luciferase-expressing plasmid (*pLuc*) or Myc-tagged wild-type ULK1 for 24 h and then analyzed for degradation of [^{14}C]valine-labeled proteins in either fully fed or 2 h starvation conditions (*EBSS*). Shown are averages ± S.D. from three independent samples. *, $p < 0.02$. *Right*, cells transfected in parallel were analyzed for expression of Myc-tagged ULK1. *C*, 293/GFP-LC3 cells were transfected with pLuc or various Myc-tagged ULK1 constructs as indicated for 24 h. Increasing amounts of DNA were used in the transfection and each condition was analyzed in duplicate. Cells were starved in EBSS/leupeptin for 2 h where indicated and analyzed by SDS-PAGE for GFP-LC3 conversion and expression of Myc-tagged ULK1. *D*, 293/GFP-LC3 cells were transfected as shown and analyzed for degradation of [^{14}C]valine labeled proteins as in *B*. Shown are averages ± S.D. from three independent samples. *, $p < 0.003$. *E–G*, 293/GFP-LC3 cells were transfected as indicated and analyzed as in *C*. In *G*, the membrane was re-probed with a polyclonal antibody for the β-COP coatomer subunit as loading control. *C*, *E*, *F*, and *G* show representative data of 2–3 independent experiments.

localization of ULK1, we examined a range of expression levels produced after transfection (see supplemental Fig. S6*A*). Wild-type ULK1, expressed at intermediate levels, is largely diffuse in the cytoplasm of starved cells but is also localized to large irregularly shaped structures that contain GFP-LC3 (supplemental Fig. S6*B*). By comparison, ULK1 expressed at lower but clearly detectable levels in starved cells was primarily cytosolic and localized to relatively smaller distinct puncta that were more uniform in size (Fig. 6*A*). These ULK1-positive puncta clearly co-localized with GFP-LC3, which labels both early and late autophagosomal structures. We reasoned that ULK1 expressed at these modest levels would best recapitulate the endogenous protein, and so our analysis of ULK1 mutants focused on cells with equivalently modest expression levels. The ULK1ΔVYA mutant in starved cells displayed a localization pattern identical to wild-type ULK1 (Fig. 6*B*). In contrast, ULK1ΔCTD, ULK1-(1–427) (data not shown) and ULK1-(1–351) were fully diffuse in the cytoplasm and did not localize to any structures (Fig. 6, *C* and *D*). These data demonstrate that the localization of ULK1 to GFP-LC3-positive cytoplasmic structures requires the C-terminal 222 amino acids of ULK1 but does not require the PDZ domain binding motif. Furthermore, membrane localization is not a prerequisite for the inhibitory function of overexpressed small N-terminal ULK1 fragments.

DISCUSSION

siRNA Screen for Modulators of Autophagy—To identify novel regulators of autophagy, we screened a siRNA library targeting 753 human kinases and associated factors using an assay that relies on quantification of GFP-LC3 lipidation after starvation. Each gene in the library was initially targeted by a "SMART" pool of 4 siRNAs. With primary data collected in duplicate, we defined lists of genes that modulated the response to amino acid starvation. When we re-screened 12 candidates by assaying individual duplexes, we found only 7 that passed the criteria of having multiple siRNAs giving the similar autophagy phenotype and transcript targeting effects. We conclude that the remaining 5 candidates most likely were identified as a result of off-target siRNA effects that affect GFP-LC3 conversion by unknown mechanisms.

Candidates—Using this screen, we have identified a number of potential candidate genes with autophagy modulatory roles and we performed a preliminary analysis of 6 candidates. At the

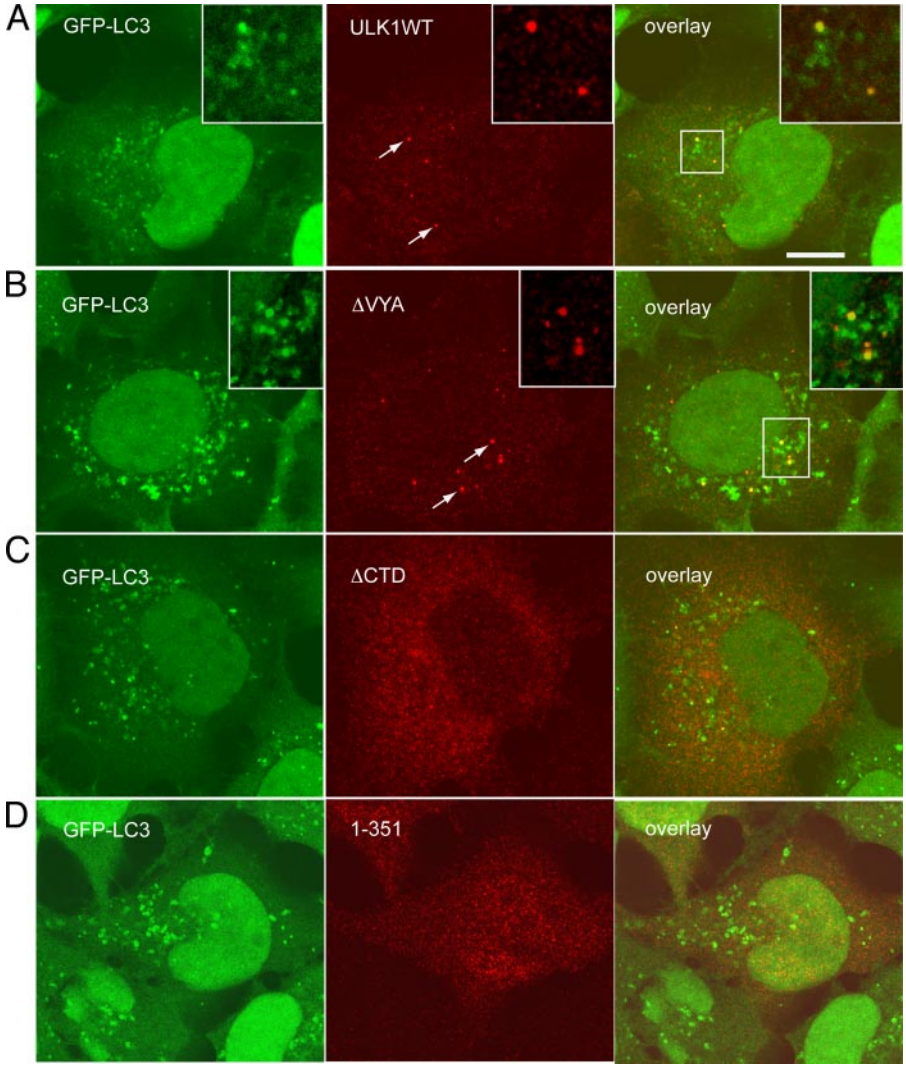

FIGURE 6. **Localization of ULK1 to GFP-LC3 structures depends on the CTD.** 293/GFP-LC3 cells were transfected with Myc-ULK1 constructs (*A*, wild type; *B*, ΔVYA; *C*, ΔCTD and *D*, 1–351) for 24 h. Cells were then starved for 2 h in EBSS/leupeptin and then fixed and stained with anti-Myc antibody. Wild-type and ΔVYA MYC-ULK1 are localized to small distinct puncta and a fraction of these co-localize with GFP-LC3 (*arrows* and *insets*). *Scale bar*, 10 μm.

level of GFP-LC3 conversion, knockdown of *CDK8*, *ROCK1*, and *LOC340371* was found to stimulate the autophagic response while knockdown of *MAP2K6*, *HUNK*, and *SGK1* was found to inhibit the autophagy response. siRNAs for the novel candidates *CDK8*, *ROCK1*, and *LOC340371* all significantly increased levels of protein degradation following starvation in 293 cells, which suggested that the respective gene products can regulate overall rates of autophagic flow. This hypothesis remains to be tested. However, because knockdown of these candidates did not activate basal autophagy, there is the alternative hypothesis that decreased function of these genes may allow cells to have a better or more sustained response once autophagy is induced.

Of the candidates that decreased GFP-LC3 conversion, only depletion of *ULK1* resulted in a significant decrease in long-lived protein degradation. The lack of inhibition of protein degradation observed after knockdown of *MAP2K6*, *HUNK*, and *SGK1* may suggest 1) the candidates inhibit only the machinery involved in lipidation of LC3, and this is not essential for long-lived protein degradation, or 2) the inhibition of lipidation reflects a kinetic delay in the process of autophagy and the overall flux through the pathway is unchanged. These hypotheses remain to be tested.

Strikingly, a number of genes were missing from the list of identified autophagy modulators. For example, mTOR, p70S6 kinase, AMPK, ERK, Akt1, DAPK, and phosphatidylinositol 3-kinases have all been implicated in the regulation of autophagy (41, 43, 51–54). Because this was an unexpected finding, we performed additional experiments on the most obvious omissions, mTOR and the two p70S6 kinase genes, and confirmed that knockdown of these genes individually did not alter starvation-induced GFP-LC3 conversion, despite effectively targeting the mTOR-p70S6 kinase signaling pathway. However, simultaneous knockdown of both p70S6 kinase genes inhibited starvation-induced GFP-LC3 conversion, which is consistent with a requirement for p70S6 kinase activity for maximal autophagy (as demonstrated in the *Drosophila* fat body) (31). As our cell line responds to rapamycin treatment, further experiments are needed to clarify the results with mTOR and p70S6 kinase siRNA. Regardless, these results underscore the fact that combined knockdown of multiple family members or components is sometimes necessary to effectively target a signaling pathway, and highlight the drawback of the library screens which target single proteins.

Knockdown of ULK1 Inhibits Autophagy—In the kinome screen, *ULK1* was identified as the most robust candidate, which provides additional proof-of-principle for the screen as a whole, since this is one of the homologues of the yeast Atg1p. In *Dictyostelium*, *Drosophila*, and *Caenorhabditis elegans*, it has been shown that *Atg1* is critical for developmental or growth regulatory processes that are dependent on autophagy (6, 7, 32). Knockdown of *ULK1* could decrease the autophagy response in multiple assays and this requirement for *ULK1* could be confirmed in two different human cell types. Knockdown of *ULK1* produced a block in the autophagy mechanism that was downstream of mTOR, consistent with the signaling pathway outlined from studies in yeast (29) and more recently *Drosophila* (31, 32). Our results here, taken together with published findings highlight the primacy of *ULK1* in autophagy. Unlike the previously described

model systems, vertebrates contain two genes, *ULK1* and *ULK2,* that encode proteins with close homology to Atg1p. Both ULK1 and ULK2 are widely expressed in mouse tissues and kinase-dead versions of ULK1 and ULK2 can act as dominant negative proteins in neurite outgrowth assays (34, 38). We found that knockdown of *ULK2* did not inhibit GFP-LC3 conversion, suggesting that only ULK1 has autophagy regulatory roles, at least in 293 cells. Using the same cell type, we recently found that ULK1 but not ULK2 is involved in a subcellular trafficking step of mammalian Atg9 that occurs when autophagy is activated by amino acid starvation or rapamycin treatment (35).

Deletion Analysis Reveals Functional Domains in ULK1—Overexpression of wild-type ULK1 in 293 cells inhibited autophagy, contrary to the recent findings that Atg1 overexpression alone in *Drosophila* could induce autophagy even under full nutrient conditions (32). This discrepancy suggests that the autophagy regulatory mechanisms involving Atg1 family proteins in *Drosophila* and human cells may be different. In our experiments, both wild-type and kinase-dead ULK1 inhibited starvation-induced autophagy in a dosage-dependent fashion to a similar extent, suggesting that the effect did not require a phosphorylation event but rather occurred by binding of other critical interacting partners. Interestingly, ULK1 lacking a conserved C-terminal region, the CTD (residues 829–1051), was a more robust dominant-negative molecule and this differential potency could be further mapped to the PDZ domain-binding VYA motif at the C terminus. These data suggest that ULK1 interaction at its C terminus with PDZ-containing proteins such as Syntenin1 (48) or other yet unidentified partners may influence its availability for binding to proteins, which would be directly involved in autophagy. Loss of interaction of ULK1 with PDZ-binding domain-containing proteins may allow internal ULK1 domains to become available to interact with other regulatory factors. Importantly, deletion of the CTD also resulted in an inhibition of long-lived protein degradation, suggesting that the inhibition is not a result of a kinetic delay, but a genuine dominant-negative effect.

The minimal region consisting of residues 1–351 was inhibitory, while the region encompassing 1–278 of ULK1 (the kinase domain) was not. This suggests that residues 279–351 of ULK1, a region that contains autophosphorylation sites (55), may contain a sequence that binds a critical autophagy regulatory component. Because no known ULK1 effector binds fragments of this size (49), other novel binding proteins yet to be identified appear to be involved in this mechanism.

The behavior of the inhibitory ULK1 fragments described here differ from those described for the Atg1 homologs in *Dictyostelium* and *Drosophila* that were converted into dominant-negative molecules through inactivation of kinase activity (32, 56). As mentioned above, in 293 cells, wild-type and K46R (kinase-inactive) ULK1 behaved similarly in terms of modulation of autophagy when overexpressed. In contrast, K46R ULK1 exhibited a dominant-inhibitory effect on outgrowth in mouse cerebellar neurons (38). Taken together, the data suggest that Atg1/ULK1 proteins may have multiple mechanisms for regulating autophagy and/or neuronal function and the contribution of each of these may vary in a cell-specific manner depending on the expression of co-regulatory molecules.

Localization of ULK1 to GFP-LC3-positive Structures Requires the C-terminal Domain—Our studies indicate that expression levels of exogenous ULK1 are an important determinant of both protein localization and autophagy regulatory function. Inhibition of autophagy was dependent on the amount of ULK1, both in cell lysates and in single cell analysis. As described above, overexpression of wild-type ULK1 in 293 cells did not induce autophagy under fed conditions, and at high levels, inhibited starvation-induced autophagy. After examination of the subcellular localization of transiently transfected ULK1, we observed in a small proportion of cells with very high levels of exogenous ULK1 (wild type and mutant) an increased prevalence of cell death which could be apoptotic or necrotic (data not shown). Cells with intermediate to high levels of overexpression showed a higher proportion with healthy morphology and in this population, the dominant-negative constructs such as ULK1ΔVYA and ULK1ΔCTD inhibited the formation of starvation-induced GFP-LC3 puncta, consistent with our biochemical analyses. In *Drosophila* imaginal discs overexpression of Atg1 led to higher levels of apoptotic cell death in addition to stimulating autophagy (32). We speculate that very high levels of ULK1 overexpression producing cell death might be mirroring the relationship between Atg1 overexpression and apoptosis observed in *Drosophila*.

ULK1, when overexpressed at high to moderate levels, formed large structures, some of which contained GFP-LC3. These structures may represent abnormal membrane compartments or alternatively, aggregated ULK1 and GFP-LC3. Importantly however, ULK1 overexpressed at low levels localized to smaller and finer structures that partially overlapped with GFP-LC3-positive puncta in starved cells. The overall appearance of this epitope tagged-ULK1 most resembled the reported structures that stained positive for endogenous ULK1 in HeLa cells (49). These ULK1 and GFP-LC3 double-positive structures might represent the mammalian equivalent of the Atg1- and Atg8-positive PAS described in yeast. Relying on a morphological analysis, we determined that deletion of the VYA motif (or the C-terminal 50 residues, data not shown) had no effect on the localization of ULK1 to small GFP-LC3-positive structures suggesting that binding of ULK1 to Syntenin or SynGAP was not involved. However, deletion of the entire CTD disrupted the localization of ULK1 to all punctate structures indicating a requirement for regions of the CTD from 829–1001 for membrane localization. In addition to mediating protein-protein interactions, the CTD has been shown to be important for neurite outgrowth inhibition by kinase-dead ULK1 (38), autophagy regulation by Atg1 in *Dictyostelium* (56) and the coordinate regulation of autophagy and CVT trafficking pathway in yeast (57). The ULK1-(1–351) minimal dominant-negative fragment was completely diffuse in the cytoplasm suggesting that the formation of inhibitory complexes was occurring in the cytosol.

Conclusion—Our search for autophagy regulators yielded a list of potential candidates and a subset of these was con-

firmed through additional validation in independent assays. The candidate ULK1 was pursued further due to its homology to yeast Atg1 and the lack of information about the role of ULK1 in autophagy. ULK1 is required for autophagy while overexpression of ULK1 also inhibits autophagy, thus allowing us to identify several ULK1 domains with important regulatory and localization functions. In conjunction with our earlier findings on ULK1 in modulating Atg9 subcellular dynamics (35), we propose that ULK1 performs an essential role for mammalian autophagy by directing membrane trafficking events in concert with the recruitment of so far unidentified regulatory molecules.

Acknowledgments—We thank Gavin Kelly for assistance with statistical analysis, Jonathan Backer for siRNA sequence information, Eeva-Liisa Eskelinen for providing cells, and Toshifumi Tomoda for ULK1 constructs.

REFERENCES

1. Komatsu, M., Waguri, S., Ueno, T., Iwata, J., Murata, S., Tanida, I., Ezaki, J., Mizushima, N., Ohsumi, Y., Uchiyama, Y., Kominami, E., Tanaka, K., and Chiba, T. (2005) *J. Cell Biol.* **169,** 425–434
2. Iwata, A., Riley, B. E., Johnston, J. A., and Kopito, R. R. (2005) *J. Biol. Chem.* **280,** 40282–40292
3. Rodriguez-Enriquez, S., He, L., and Lemasters, J. J. (2004) *Int. J. Biochem. Cell Biol.* **36,** 2463–2472
4. Ravikumar, B., Vacher, C., Berger, Z., Davies, J. E., Luo, S., Oroz, L. G., Scaravilli, F., Easton, D. F., Duden, R., O'Kane, C. J., and Rubinsztein, D. C. (2004) *Nat. Genet.* **36,** 585–595
5. Kuma, A., Hatano, M., Matsui, M., Yamamoto, A., Nakaya, H., Yoshimori, T., Ohsumi, Y., Tokuhisa, T., and Mizushima, N. (2004) *Nature* **432,** 1032–1036
6. Melendez, A., Talloczy, Z., Seaman, M., Eskelinen, E. L., Hall, D. H., and Levine, B. (2003) *Science* **301,** 1387–1391
7. Otto, G. P., Wu, M. Y., Kazgan, N., Anderson, O. R., and Kessin, R. H. (2004) *J. Biol. Chem.* **279,** 15621–15629
8. Lum, J. J., Bauer, D. E., Kong, M., Harris, M. H., Li, C., Lindsten, T., and Thompson, C. B. (2005) *Cell* **120,** 237–248
9. Shimizu, S., Kanaseki, T., Mizushima, N., Mizuta, T., Arakawa-Kobayashi, S., Thompson, C. B., and Tsujimoto, Y. (2004) *Nat Cell Biol.* **6,** 1221–1228
10. Daido, S., Kanzawa, T., Yamamoto, A., Takeuchi, H., Kondo, Y., and Kondo, S. (2004) *Cancer Res.* **64,** 4286–4293
11. Scarlatti, F., Bauvy, C., Ventruti, A., Sala, G., Cluzeaud, F., Vandewalle, A., Ghidoni, R., and Codogno, P. (2004) *J. Biol. Chem.* **279,** 18384–18391
12. Boya, P., Gonzalez-Polo, R. A., Casares, N., Perfettini, J. L., Dessen, P., Larochette, N., Metivier, D., Meley, D., Souquere, S., Yoshimori, T., Pierron, G., Codogno, P., and Kroemer, G. (2005) *Mol. Cell. Biol.* **25,** 1025–1040
13. Qu, X., Yu, J., Bhagat, G., Furuya, N., Hibshoosh, H., Troxel, A., Rosen, J., Eskelinen, E. L., Mizushima, N., Ohsumi, Y., Cattoretti, G., and Levine, B. (2003) *J. Clin. Investig.* **112,** 1809–1820
14. Yue, Z., Jin, S., Yang, C., Levine, A. J., and Heintz, N. (2003) *Proc. Natl. Acad. Sci. U. S. A.* **100,** 15077–15082
15. Gutierrez, M. G., Master, S. S., Singh, S. B., Taylor, G. A., Colombo, M. I., and Deretic, V. (2004) *Cell* **119,** 753–766
16. Ogawa, M., Yoshimori, T., Suzuki, T., Sagara, H., Mizushima, N., and Sasakawa, C. (2005) *Science* **307,** 727–731
17. Thumm, M., Egner, R., Koch, B., Schlumpberger, M., Straub, M., Veenhuis, M., and Wolf, D. H. (1994) *FEBS Lett.* **349,** 275–280
18. Tsukada, M., and Ohsumi, Y. (1993) *FEBS Lett.* **333,** 169–174
19. Klionsky, D. J., Cregg, J. M., Dunn, W. A., Jr., Emr, S. D., Sakai, Y., Sandoval, I. V., Sibirny, A., Subramani, S., Thumm, M., Veenhuis, M., and Ohsumi, Y. (2003) *Dev. Cell* **5,** 539–545
20. Suzuki, K., Kirisako, T., Kamada, Y., Mizushima, N., Noda, T., and Ohsumi, Y. (2001) *EMBO J.* **20,** 5971–5981
21. Mizushima, N., Yamamoto, A., Hatano, M., Kobayashi, Y., Kabeya, Y., Suzuki, K., Tokuhisa, T., Ohsumi, Y., and Yoshimori, T. (2001) *J. Cell Biol.* **152,** 657–668
22. Kirisako, T., Ichimura, Y., Okada, H., Kabeya, Y., Mizushima, N., Yoshimori, T., Ohsumi, M., Takao, T., Noda, T., and Ohsumi, Y. (2000) *J. Cell Biol.* **151,** 263–276
23. Kuma, A., Mizushima, N., Ishihara, N., and Ohsumi, Y. (2002) *J. Biol. Chem.* **277,** 18619–18625
24. Ichimura, Y., Kirisako, T., Takao, T., Satomi, Y., Shimonishi, Y., Ishihara, N., Mizushima, N., Tanida, I., Kominami, E., Ohsumi, M., Noda, T., and Ohsumi, Y. (2000) *Nature* **408,** 488–492
25. Kabeya, Y., Mizushima, N., Ueno, T., Yamamoto, A., Kirisako, T., Noda, T., Kominami, E., Ohsumi, Y., and Yoshimori, T. (2000) *EMBO J.* **19,** 5720–5728
26. Mizushima, N., Yamamoto, A., Matsui, M., Yoshimori, T., and Ohsumi, Y. (2004) *Mol. Biol. Cell* **15,** 1101–1111
27. Kochl, R., Hu, X. W., Chan, E. Y., and Tooze, S. A. (2006) *Traffic* **7,** 129–145
28. Kuma, A., Matsui, M., and Mizushima, N. (2007) *Autophagy* **3,** 323–328
29. Kamada, Y., Funakoshi, T., Shintani, T., Nagano, K., Ohsumi, M., and Ohsumi, Y. (2000) *J. Cell Biol.* **150,** 1507–1513
30. Budovskaya, Y. V., Stephan, J. S., Deminoff, S. J., and Herman, P. K. (2005) *Proc. Natl. Acad. Sci. U. S. A.* **102,** 13933–13938
31. Scott, R. C., Schuldiner, O., and Neufeld, T. P. (2004) *Dev Cell* **7,** 167–178
32. Scott, R. C., Juhasz, G., and Neufeld, T. P. (2007) *Curr. Biol.* **17,** 1–11
33. Kuroyanagi, H., Yan, J., Seki, N., Yamanouchi, Y., Suzuki, Y., Takano, T., Muramatsu, M., and Shirasawa, T. (1998) *Genomics* **51,** 76–85
34. Yan, J., Kuroyanagi, H., Tomemori, T., Okazaki, N., Asato, K., Matsuda, Y., Suzuki, Y., Ohshima, Y., Mitani, S., Masuho, Y., Shirasawa, T., and Muramatsu, M. (1999) *Oncogene* **18,** 5850–5859
35. Young, A. R., Chan, E. Y., Hu, X. W., Kochl, R., Crawshaw, S. G., High, S., Hailey, D. W., Lippincott-Schwartz, J., and Tooze, S. A. (2006) *J. Cell Sci.* **119,** 3888–3900
36. Lee, S. B., Kim, S., Lee, J., Park, J., Lee, G., Kim, Y., Kim, J. M., and Chung, J. (2007) *EMBO Rep.* **8,** 360–365
37. Zhou, X., Babu, J. R., da Silva, S., Shu, Q., Graef, I. A., Oliver, T., Tomoda, T., Tani, T., Wooten, M. W., and Wang, F. (2007) *Proc. Natl. Acad. Sci. U. S. A.* **104,** 5842–5847
38. Tomoda, T., Bhatt, R. S., Kuroyanagi, H., Shirasawa, T., and Hatten, M. E. (1999) *Neuron* **24,** 833–846
39. Liang, X. H., Jackson, S., Seaman, M., Brown, K., Kempkes, B., Hibshoosh, H., and Levine, B. (1999) *Nature* **402,** 672–676
40. Ogier-Denis, E., Houri, J. J., Bauvy, C., and Codogno, P. (1996) *J. Biol. Chem.* **271,** 28593–28600
41. Ogier-Denis, E., Pattingre, S., El Benna, J., and Codogno, P. (2000) *J. Biol. Chem.* **275,** 39090–39095
42. Smyth, G. K. (2004) *Stat. Appl. Genet. Mol. Biol.* **3,** Article 3
43. Blommaart, E. F., Luiken, J. J., Blommaart, P. J., van Woerkom, G. M., and Meijer, A. J. (1995) *J. Biol. Chem.* **270,** 2320–2326
44. Kihara, A., Kabeya, Y., Ohsumi, Y., and Yoshimori, T. (2001) *EMBO Rep.* **2,** 330–335
45. Moffat, J., Reiling, J. H., and Sabatini, D. M. (2007) *Trends Pharmacol. Sci.* **28,** 149–151
46. Houri, J. J., Ogier-Denis, E., Trugnan, G., and Codogno, P. (1993) *Biochem. Biophys. Res. Commun.* **197,** 805–811
47. Mavrakis, M., Lippincott-Schwartz, J., Stratakis, C. A., and Bossis, I. (2006) *Hum. Mol. Genet.* **15,** 2962–2971
48. Tomoda, T., Kim, J. H., Zhan, C., and Hatten, M. E. (2004) *Genes Dev.* **18,** 541–558
49. Okazaki, N., Yan, J., Yuasa, S., Ueno, T., Kominami, E., Masuho, Y., Koga, H., and Muramatsu, M. (2000) *Brain Res. Mol. Brain Res.* **85,** 1–12
50. Kim, J., Huang, W. P., Stromhaug, P. E., and Klionsky, D. J. (2002) *J. Biol. Chem.* **277,** 763–773
51. Arico, S., Petiot, A., Bauvy, C., Dubbelhuis, P. F., Meijer, A. J., Codogno, P., and Ogier-Denis, E. (2001) *J. Biol. Chem.* **276,** 35243–35246
52. Samari, H. R., Moller, M. T., Holden, L., Asmyhr, T., and Seglen, P. O.

(2005) *Biochem. J.* **386,** 237–244
53. Inbal, B., Bialik, S., Sabanay, I., Shani, G., and Kimchi, A. (2002) *J. Cell Biol.* **157,** 455–468
54. Blommaart, E. F., Krause, U., Schellens, J. P., Vreeling-Sindelarova, H., and Meijer, A. J. (1997) *Eur. J. Biochem.* **243,** 240–246
55. Yan, J., Kuroyanagi, H., Kuroiwa, A., Matsuda, Y., Tokumitsu, H., Tomoda, T., Shirasawa, T., and Muramatsu, M. (1998) *Biochem. Biophys. Res. Commun.* **246,** 222–227
56. Tekinay, T., Wu, M. Y., Otto, G. P., Anderson, O. R., and Kessin, R. H. (2006) *Eukaryot Cell* **5,** 1797–1806
57. Abeliovich, H., Zhang, C., Dunn, W. A., Jr., Shokat, K. M., and Klionsky, D. J. (2003) *Mol. Biol. Cell* **14,** 477–490